Transition from insulating to metallic phase induced by in-plane magnetic field in HgTe quantum wells

G. M. Gusev,[1] E. B. Olshanetsky,[2] Z. D. Kvon,[2,3] O. E. Raichev,[4] N. N. Mikhailov,[2] and S. A. Dvoretsky[2]
[1]*Instituto de Física da Universidade de São Paulo, 135960-170 São Paulo, SP, Brazil*
[2]*Institute of Semiconductor Physics, Novosibirsk 630090, Russia*
[3]*Novosibirsk State University, Novosibirsk 630090, Russia*
[4]*Institute of Semiconductor Physics, NAS of Ukraine, Prospekt Nauki 41, 03028 Kiev, Ukraine*
(Received 13 March 2013; revised manuscript received 15 July 2013; published 14 November 2013)

We report transport measurements in HgTe-based quantum wells with well width of 8 nm, corresponding to the quantum spin Hall state, subject to in-plane magnetic field. In the absence of the magnetic field the local and nonlocal resistances behave very similarly, which confirms the edge state transport in our system. In the magnetic field, we observe a monotonic decrease of the resistance with saturation of local resistance, while nonlocal resistance disappears completely, independent of the gate voltage. We believe that this evidence of metallic behavior indicates a transition to a gapless two-dimensional phase, according to theoretical predictions. The influence of disorder on resistivity properties of HgTe quantum wells under in-plane magnetic field is discussed.

DOI: 10.1103/PhysRevB.88.195305 PACS number(s): 73.43.Qt, 73.40.Qv

I. INTRODUCTION

Recent years have witnessed an astonishing growth in research on topological insulators, the materials that have a bulk band gap like an ordinary insulator but support conducting states on their edge or surface.[1–7] The two-dimensional (2D) topological insulators can be classified either into quantum Hall effect (QHE) state or quantum spin Hall effect (QSHE) state. The edge modes in the traditional integer quantum Hall system are chiral because time-reversal symmetry is broken by the magnetic field. In contrast, the QSHE state is described by pairs of counterpropagating edge modes with opposite spin polarizations (Kramers pairs) so that the time-reversal symmetry is maintained. Experimentally measured 4-probe resistance in a micrometer-sized Hall bar fabricated from HgTe/CdHgTe quantum well structure demonstrates a quantized plateau $R_{xx} \simeq h/2e^2$ in the absence of a perpendicular magnetic field.[8] This fact, supported by a theoretical consideration of the possibility of the QSHE regime in HgTe quantum wells,[7] has been taken as definitive evidence for the QSHE state. One more experimental piece of evidence for QSHE is a nonlocal transport,[9] when application of the current between a pair of contacts creates a net current along the sample edge and causes a voltage at any other pair of the contacts. In the QHE regime, when the edge modes are chiral, the nonlocal response requires backscattering between opposite edges, which occurs via the bulk states and disappears at purely integer filling of Landau levels. In the QSHE state, the nonlocal response always exists because of the presence of two counterpropagating edge modes at the same edge. Moreover, the spin-flip scattering between these modes, which is important in HgTe quantum well structures of several micrometer size,[8] makes the nonlocal resistance considerably larger than the resistance quantum.[10]

A remarkable property of HgTe quantum wells is the opportunity to create different band structures for 2D electrons. The ordinary 2D insulator state is realized at small well widths (approximately, up to 6.3 nm), while the 2D topological insulator (QSHE) state exists at larger well widths. The large-width (20 nm and wider) quantum wells support a semimetallic 2D state[11–13] with overlapped conduction and valence 2D bands. Recent theoretical consideration[14] suggests one more possibility, when application of a strong (of the order 10 T) magnetic field parallel to the plane of HgTe quantum well in the QSHE state rebuilds the subband structure and creates a gapless 2D state with electron energy spectrum similar to that of bulk HgTe. Preliminary experimental studies[10] indeed show a strong decrease of the resistance of HgTe quantum well structures with increasing in-plane magnetic field above 10 T, which can be a signature of a transition to metallic state. Since the problem of this phase transition deserves more attention, we have carried out additional experiments and theoretical calculations. The nonlocal resistance measurements are very useful for this purpose, because the appearance of the metallic state in the bulk of the sample shunts the edge channel transport and makes the nonlocal resistance exponentially small, practically equal to zero.

In this paper we present results of resistance measurements in 8-nm-wide wells of different sizes in the presence of the in-plane magnetic field. The four-terminal resistance in samples with gate size 13×7 μm^2 is $R_{xx} \simeq 300$ kΩ and still significantly larger than $h/2e^2$. The nonlocal transport experiments with these devices in the QSHE regime demonstrate that charge transport occurs through extended edge channels. Experimentally, we show that the in-plane magnetic field suppresses nonlocal resistance completely, while local transport demonstrates a monotonic decrease of the resistance with saturation. The evolution of the 2D subband structure with increasing magnetic field is calculated by means of numerical solution of the eigenstate problem for the 6×6 matrix Kane Hamiltonian taking into account strain effects in HgTe well. These calculations confirm the gapless nature of the metallic state induced by the magnetic field. To describe the behavior of the resistance near the phase transition, we analyze the influence of smooth inhomogeneities of the system such as variations of the well width and electrostatic potential.

The paper is organized as follows. In Sec. II we characterize the samples and present the results of resistance measurements in zero magnetic field. Section III describes experimental results in parallel magnetic field. A theoretical analysis is

 ©2013 American Physical Society

presented in Sec. IV. The final section contains a brief discussion of the results.

II. EXPERIMENT IN ZERO MAGNETIC FIELD

The $Cd_{0.65}Hg_{0.35}Te/HgTe/Cd_{0.65}Hg_{0.35}Te$ quantum wells with [013] surface orientations and widths of 8–8.3 nm were prepared by molecular beam epitaxy. The sample consists of three 5-μm-wide consecutive segments of different length (6.5, 20, 6.5 μm), and 8 voltage probes. The ohmic contacts to the two-dimensional gas were formed by the in-burning of indium. To prepare the gate, a dielectric layer containing 100 nm SiO_2 and 200 nm Si_3Ni_4 was first grown on the structure using the plasmochemical method. Then, the TiAu gate was deposited. We present experimental results on three different type of the devices, which are schematically shown in Fig. 1. Device A [Fig. 1(a)] is a structure with large gate area for identifying nonlocal transport over macroscopic distances.[10] The lengths of the edge states are determined by the perimeter of the sample part covered by a metallic gate (mostly side branches) rather than by the length of the bar itself. Devices B and C are structures with small gate area. Device B is designed for multiterminal measurements, while device C has been used for two-terminal measurements. Several devices with the same configuration have been studied. The density variation with gate voltage was 1.09×10^{11} cm^{-2} V^{-1}. The electron mobility exhibits nonmonotonic dependence on the carrier density with distinct maximum $\mu_n = 250 \times 10^3$ cm^{-2}/V s at $n_s = 2 \times 10^{11}$ cm^{-2}, and hole mobility demonstrates a saturation $\mu_p = 20 \times 10^3$ cm^{-2}/V s with carrier density $p_s = 1.5 \times 10^{11}$ cm^{-2}. The magnetotransport measurements in the described structures were performed in the temperature range from 1.4 K to 25 K and in magnetic fields up to 12 T using a standard four-point circuit with a 3–13 Hz ac input of 0.1–10 nA through the sample, which is sufficiently low to avoid the overheating effects.

The carrier density in HgTe quantum wells can be electrically manipulated with the gate voltage V_g. The typical dependence of the four-terminal local $R_{I=1,4;V=2,3}$ and nonlocal $R_{I=6,2;V=5,3}$ resistances as a function of V_g in device A [Fig. 1(a)] exhibits a sharp peak that is $\sim 10^4$ times greater than the resistance at $V_g \sim 2$ V far from the peak position. The Hall coefficient reverses its sign when R_{xx} approaches its maximum value.[10] This behavior resembles the ambipolar field effect observed in graphene.[15] Thus, the gate voltage alters the quantum wells from n-type conductor to p-type conductor via an insulating state. The nonlocal resistance $R_{I=6,2;V=5,3}$ in the insulating regime has a comparable amplitude and qualitatively the same position and width of the peak as the local resistance. Outside of the peak the nonlocal resistance is negligibly small, as expected for the conducting state. Figures 1(b) and 1(c) show the experimental data for devices B and C. One can see that the peak resistance is dramatically reduced in the samples of a few micrometer size, but it is still far higher than the resistance in the ballistic edge state transport regime. Based on the conductance of $0.1e^2/h$ for a 3–6 micrometer long sample, one may conclude that the ballistic regime in our samples is expected if we reduce the sample length to less than ~ 0.5 μm. The understanding of

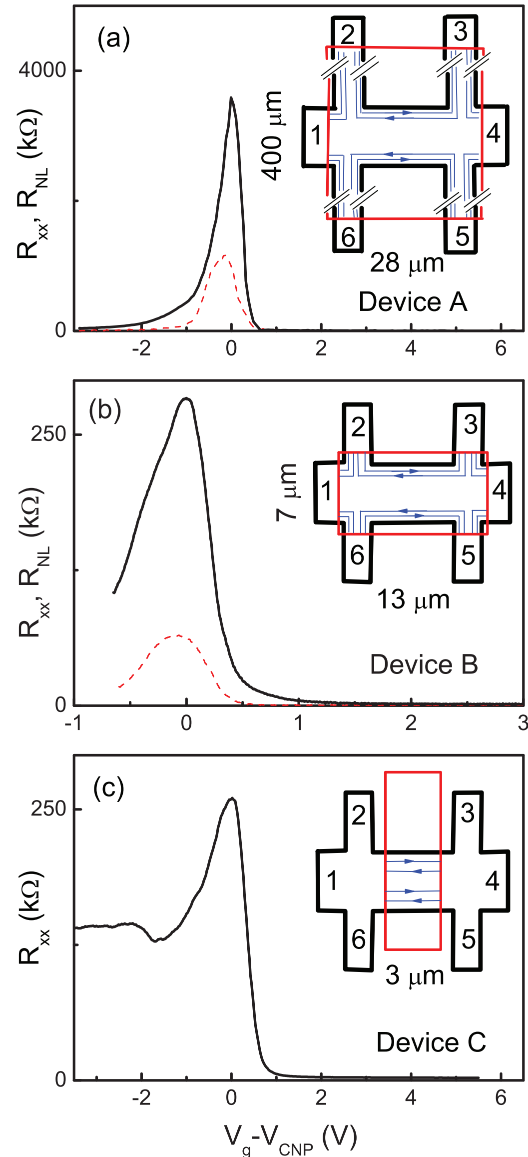

FIG. 1. (Color online) Four-terminal local $R_{I=1,4;V=2,3}$ (black) and nonlocal $R_{I=6,2;V=5,3}$ (red dashes) resistances as a function of the gate voltage at $T = 4.2$ K and $B = 0$ for the Hall bar devices A (a), B (b), and C (c) with dimensions of the gate (length and width) indicated. The numbers indicate the coding of the leads.

the absence of the quantized transport in macroscopic samples requires further investigation.

The nonlocal resistance is different in a slightly modified configuration, where the current passes through the contacts 1 and 6 and the voltage is measured between the contacts 5 and 3. Figure 2 shows curves for three possible configurations of nonlocal resistance. The resistance is reduced when the current path is shorter, which is expected for edge state transport with backscattering. Conductivity of a 2D topological insulator is determined by a 1D channel (ballistic or diffusive), which connects all contacts (probes) at the periphery of the sample. Application of the current between any pair of contacts produces the current circulating along the entire edge. In particular, for nonlocal configuration $R_{I=6,2;V=5,3}$, which is shown in Fig. 2, two paths lead from the contact

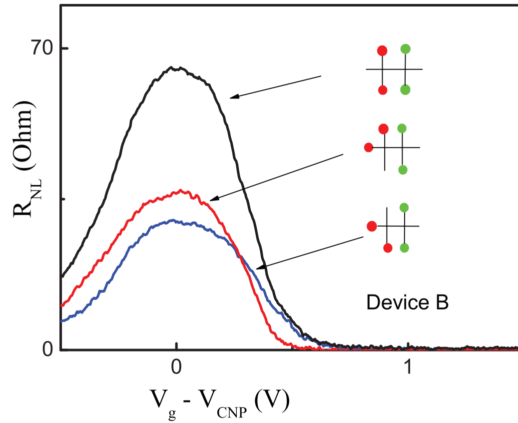

FIG. 2. (Color online) Nonlocal resistance as a function of the gate voltage for the Hall bar device B and different nonlocal configurations (from top to bottom): $R_{I=6,2;V=3,5}$, $R_{I=1,2;V=3,5}$, and $R_{I=1,6;V=3,5}$, at $T = 4.2$ K and $B = 0$.

2 to the contact 6, one (2-3,3-4,5-6) three times longer than the other (2-1,1-6). The resistance between the contacts can be substituted by the quantum resistance $R = h/2e^2$ in the ballistic case or by

$$R = \frac{h}{2e^2}(1 + \gamma L) \tag{1}$$

in the diffusive case, where γ^{-1} is the mean free path for 1D backscattering and L is the length of the 1D channel between the voltage probes. Within this approximation one would expect the following ratios between local and nonlocal resistances: $R_{I=1,4;V=2,3}/R_{I=6,2;V=5,3} \approx 0.22$; $R_{I=1,4;V=2,3}/R_{I=1,2;V=5,3} \approx 0.11$, which roughly agrees with experimental data shown in Fig. 2.

III. EXPERIMENT IN PARALLEL MAGNETIC FIELD

Applying a strong magnetic field parallel to a quantum well may lead to several effects. First, the magnetic field creates an electronic spin polarization, leading to an increase in spin scattering and an increase in resistivity.[16] Second, the parallel magnetic field leads to mixing of 2D subband states due to magneto-orbital coupling with the field, because the wave functions of the confined states have finite widths determined by the width of the well; see Ref. 17 and, in application to HgTe wells, Ref. 14.

Figure 3 shows the evolution of the local magnetoresistance with gate voltage in the presence of the in-plane magnetic field for three different devices. One can see that the resistance in the peak in magnetic fields higher than 5 T demonstrates a rapid monotonic decrease in all samples. This behavior corresponds to a transition from the insulating state to the gapless metallic state (see details in Sec. IV). With increasing gate voltage, the Fermi level is lifted up into the conduction band so the system is in the metallic state already at zero magnetic field. The resistance in this case becomes almost insensitive to the magnetic field, as expected. However, a weak positive magnetoresistance is present above a critical voltage in the short devices B and C. Surprisingly, this critical voltage is independent of the in-plane magnetic field and the corresponding resistance is of the order of the resistance quantum. We have no explanation of this particular observation.

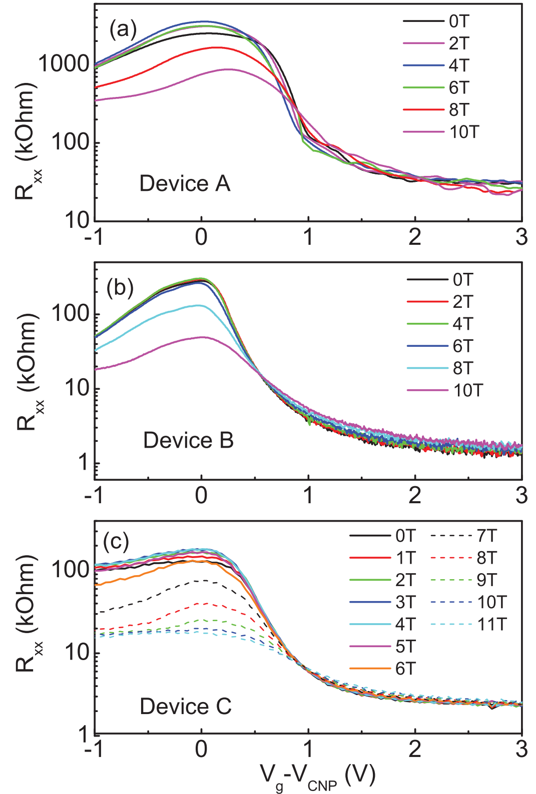

FIG. 3. (Color online) Four-terminal local $R_{I=1,4;V=2,3}$ resistance as a function of the gate voltage for the Hall bar devices and for different parallel magnetic fields, $T = 4.2$ K.

In Figs. 4 and 5 we present the magnetic-field dependence of the local and nonlocal resistances near the peak point for different temperatures for both devices A and B. One can see a monotonic decrease of the resistance with saturation of local resistance, while nonlocal resistance disappears completely above magnetic field $B \simeq 12$ T. A rapid decrease of the resistances starts approximately at $B \simeq 7$ T. In Fig. 5 one can see that the temperature effect on local resistance is weak.

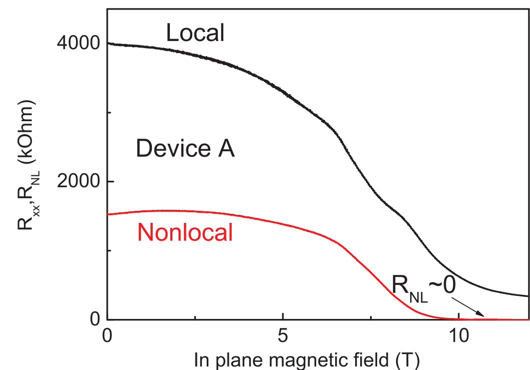

FIG. 4. (Color online) (a) The local $R_{xx} = R_{I=1,4;V=6,5}$ and nonlocal $R_{I=2,6;V=5,3}$ resistances as a function of in-plane magnetic field for device A at $V_g = -3.63$ V, T = 1.5 K. The gate voltage corresponds to the resistance peak. The nonlocal resistance disappears at $B > 10$ T.

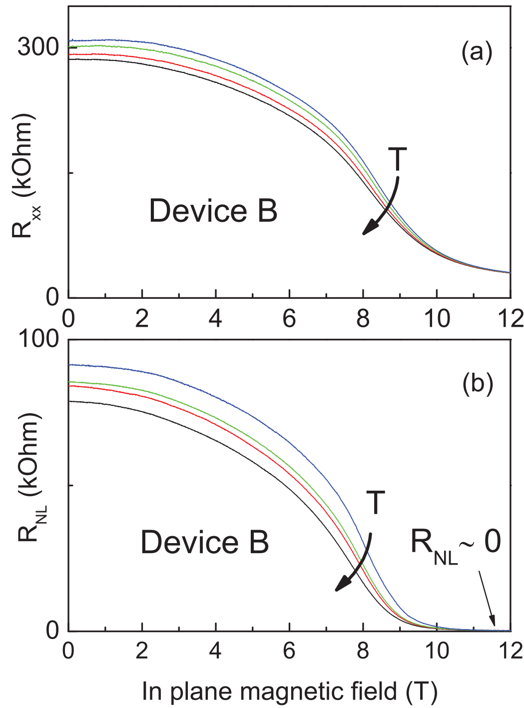

FIG. 5. (Color online) (a) The local resistance $R_{I=1,2;V=3,5}$ as a function of in-plane magnetic field for different temperatures T (K): 1.5, 2.5, 3.5, 4.2 at $V_g = -2.43$ V. (b) The nonlocal resistance $R_{I=2,6;V=5,3}$ as a function of in-plane magnetic field for different temperatures T (K): 1.5, 3, 3.6, 4.2 at $V_g = -2.4$ V. The gate voltage corresponds to the resistance peak. The nonlocal resistance disappears at $B = 12$ T.

The evolution of nonlocal resistance as a function of the gate voltage with increasing in-plane magnetic field is given in Fig. 6. For the voltages corresponding to the insulating state, we find as much as three orders of resistance reduction in $B \simeq 12$ T. The resistance peaks are asymmetric, showing a more rapid decrease with V_g in the n-type region.

Based on our experimental observations we may conclude that the external parallel magnetic field strongly suppresses local and completely destroys nonlocal resistance. The nonlocal resistance could be negligibly small in the presence of a dissipative transport in the bulk of the sample. Therefore it would be natural to assume that the in-plane magnetic field produces conducting states in the bulk and, possibly, suppresses the edge state transport. Alternatively, we may attribute zero nonlocal resistance to formation of chiral edge channels similar to the QHE state in perpendicular magnetic field. Such channels indeed are dissipationless, and the voltage drop between the contacts is zero. However, within this scenario, the local resistance would be zero as well, which disagrees with our observation. Furthermore, we do not observe any Hall resistance as the in-plane magnetic field increases.

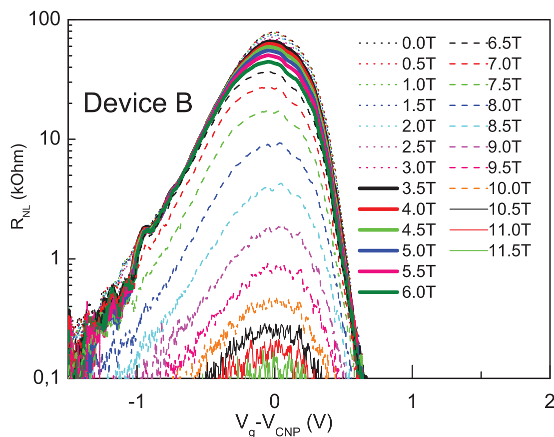

FIG. 6. (Color online) The nonlocal $R_{I=1,2;V=3,5}$ resistance as a function of gate voltage for different magnetic fields, $T = 4.2$ K.

We explain the observed suppression of nonlocal resistance as a consequence of a magnetic-field-induced phase transition from the insulating (QSHE) phase to a metallic 2D phase. Below we justify this assumption by a theoretical analysis of the 2D electron spectrum.

IV. THEORY

The phase transition from the insulating to the gapless state has been described in Ref. 14 by using the effective 2D Hamiltonian derived in the basis including one interface-like state (e) formed by hybridization of conduction electrons with light holes in the quantum well and two states corresponding to the first subbands of heavy holes (h1 and h2). As the effective Hamiltonian is valid only in a narrow region of 2D electron wave vectors near $\mathbf{k} = 0$, it is necessary to do more detailed calculations of the energy spectrum, which are not restricted by the limitations of the effective Hamiltonian approach and are nonperturbative with respect to the magnitude of B. To find the 2D electron spectrum, we have carried out a numerical solution of eigenstate problem for the 6×6 matrix Kane Hamiltonian which satisfactorily describes HgTe/CdHgTe heterostructures. We also have included the effect of uniaxial strain in the HgTe well due to the lattice mismatch of HgTe and CdHgTe. The material parameters used for these calculations are given in Ref. 13. The results for symmetric $Cd_{0.65}Hg_{0.35}Te/HgTe/Cd_{0.65}Hg_{0.35}Te$ quantum wells of width 8 nm grown along the [001] direction are shown in Figs. 7 and 8. The energy in these figures is counted from the valence band extremum in bulk HgTe.

Figure 7 demonstrates the effect of magnetic field below the point of phase transition. Three subbands (e, h1, and h2) are spin degenerate at $B = 0$, since the well is symmetric. As the subband structure is inverted (subband e is below subband h1), the system is in the QSHE state. The subband h1 forms the 2D conduction band, which is almost isotropic. The 2D valence band, formed by e and h2 subbands, shows a weak anisotropy originating from the anisotropy of hole states in bulk HgTe as the Luttinger parameters γ_2 and γ_3 are not equal to each other. The hybridization of e and h2 subbands at finite 2D wave vector k leads to anticrossing of these subbands so that an additional gap is formed within the 2D valence band. The spectrum of edge states is shown schematically, based on effective Hamiltonian calculations.[14] As the magnetic field is applied, all the subbands show spin splitting, so instead of three there are six spectral branches. The h1 state, whose wave function is symmetric at $k = 0$, remains spin degenerate at $k = 0$. The branches of the 2D valence band have a much

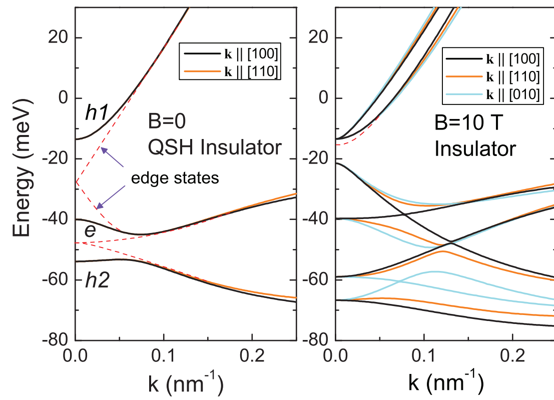

FIG. 7. (Color online) Dependence of electron energy on 2D wave number k calculated for [001]-grown 8-nm-wide symmetric quantum wells $Cd_{0.65}Hg_{0.35}Te/HgTe/Cd_{0.65}Hg_{0.35}Te$ at zero magnetic field and under in-plane magnetic field $B = 10$ T directed along [100]. Dashed lines schematically show edge state spectrum.

higher anisotropy since the spectrum becomes strongly sensitive to the direction between **k** and **B**. In the field of 10 T, the system is still in the insulating state but the gap is reduced to approximately 8 meV. The edge states do not disappear, though their spectrum is considerably modified[14] and is no longer gapless.

Figure 8 shows the spectrum at the transition field, which is equal to approximately 13.8 T for the chosen structure and is almost insensitive to interface orientation (for [013]-grown wells studied in our experiment the transition field varies from 13.6 T to 14 T depending on direction of **B** in the plane), and at a higher field of 18 T. For clarity, only one direction of **k** is shown, as for the other directions the picture is qualitatively similar. The state when the gap disappears is characterized by two linear branches forming a "Dirac cone" 2D spectrum similar to that of graphene and a third, parabolic branch passing through the Dirac point. Further increase in B does not open a gap: the system remains in the gapless state because the upper spin branch of the h1 subband is inverted and acquires a negative effective mass. Above the point of phase transition,

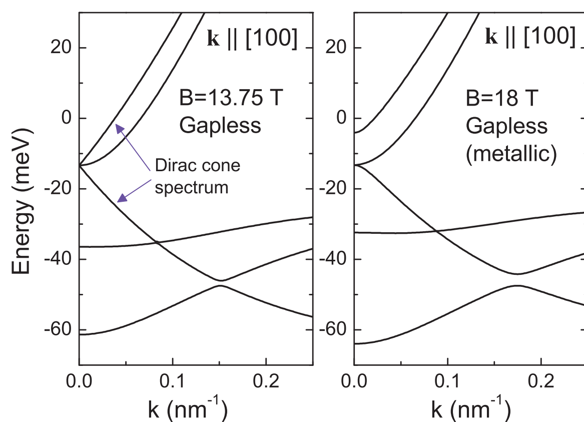

FIG. 8. (Color online) Dependence of electron energy on 2D wave number k calculated for [001]-grown 8-nm-wide symmetric quantum wells $Cd_{0.65}Hg_{0.35}Te/HgTe/Cd_{0.65}Hg_{0.35}Te$ at the transition field $B = 13.75$ T and at $B = 18$ T. Both **B** and **k** are directed along [100]. Above the transition field the spectrum is gapless.

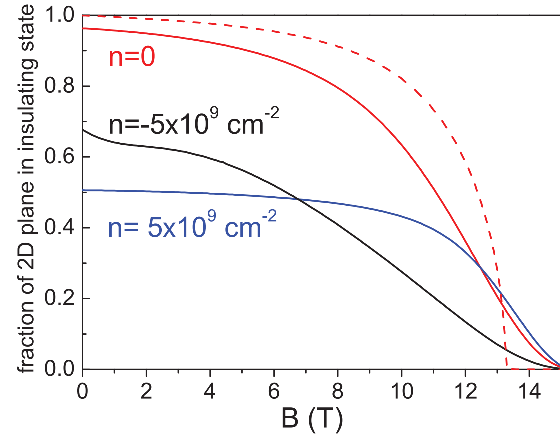

FIG. 9. (Color online) Magnetic-field dependence of the fraction of 2D plane covered by insulator for spatially inhomogeneous 8-nm-wide symmetric quantum wells $Cd_{0.65}Hg_{0.35}Te/HgTe/Cd_{0.65}Hg_{0.35}Te$ (see text for details). The dashed line shows the result where only well width variations are taken into account.

the 2D system is always in the metallic state, without regard to electron density.

The above calculations suggest an abrupt drop of both local and nonlocal resistance as the magnetic field reaches the transition field. The experiment, however, shows a smoother decrease of resistance over a wide region of magnetic fields, and nonlocal resistance disappears at a field smaller than the calculated transition field. This is not surprising, because the calculations are carried out for an ideal quantum well, while realistic quantum wells are inhomogeneous. The most important kind of spatial disorder for HgTe wells is the variation of the well width which causes energy fluctuations of all 2D subbands and variation of the insulating gap over the 2D plane. Assuming that such variations are smooth on the quantum length scale, one may use local well width a to calculate the energy spectrum and average the results over the well width distribution. For the regions with smaller gap the transition to metallic state occurs at weaker magnetic fields. Therefore, even when the magnetic field is below the transition field for a given average well width $\overline{a}$, a part of the 2D plane is already in the gapless state: a number of metallic clusters (islands) is formed. With increasing field, the average size of metallic coverage increases. This occurs not only because a larger fraction of the 2D plane is transferred into the gapless state (which is always metallic independent of Fermi energy), but also because the position of the Fermi energy, dictated by the *average* electron density n, is shifted out of the gap for some part of gapped regions of the plane. Assuming a Gaussian well width distribution $W(a) = \exp[-(a-\overline{a})^2/\delta a^2]/(\sqrt{\pi}\delta a)$ with $\delta a = 1$ nm, we have calculated the fraction of the insulating coverage of the 2D plane as a function of the magnetic field. The result for charge neutrality point ($n = 0$) is presented in Fig. 9 by the dashed line. Solid lines, plotted also for small positive and negative n, show the results calculated with an additional kind of disorder, smooth spatial fluctuations of electrostatic potential which lead to variation of the subband energies without affecting the gaps between the subbands. This disorder, usually caused in quantum wells by remote charged impurities, should be also important in view of negligible

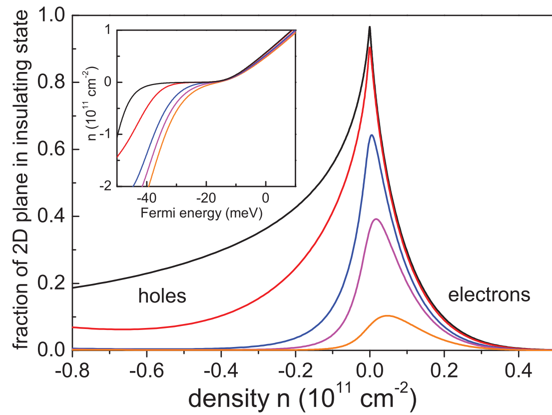

FIG. 10. (Color online) Fraction of 2D plane covered by insulator as function of electron density for spatially inhomogeneous 8-nm-wide symmetric quantum wells $Cd_{0.65}Hg_{0.35}Te/HgTe/Cd_{0.65}Hg_{0.35}Te$. The plots are taken for in-plane magnetic fields $B = 0$, 5, 10, 12, and 14 T (from top to bottom). The inset shows the dependence of electron density on Fermi energy for the given set of magnetic fields.

screening of the potential at small electron densities. To bring the inhomogeneous electrostatic potential φ into our calculations, we again use the Gaussian distribution $W(\varphi)$ with $\delta\varphi = 5$ meV.

Figure 9 demonstrates how the insulating coverage of the sample becomes smaller as the in-plane magnetic field increases. The presence of inhomogeneous electrostatic potential makes this behavior smoother but does not affect the picture qualitatively. Accordingly, the metallic coverage p becomes larger so the metallic clusters are able to further interconnect to achieve the percolation process and eventually evolve into a metallic continuum. A similar physical situation takes place when metallic films are condensed on an insulating substrate.[18] Even if the inhomogeneous electrostatic potential is neglected, almost half of the 2D plane is in the metallic state already at 12 T, and the presence of the electrostatic potential increases the metallic coverage at this magnetic field. Since different 2D models suggest a percolation threshold around $p = 0.5$ (see Ref. 19 and references therein) one may conclude that the in-plane magnetic field of about 12 T is indeed capable of inducing the phase transition to metallic state which we detect in our experiment by the disappearance of the nonlocal resistance. We also note an obvious correlation between the magnetic-field dependence of resistance shown in Figs. 4 and 5 and the behavior shown in Fig. 9.

The fraction of insulating coverage of the sample is highly sensitive to the electron density which is varied in our experiment proportional to the gate voltage. Figure 10 shows the density dependence of the insulating coverage at different magnetic fields, calculated by taking into account variations of both well width and electrostatic potential. The inset shows how the electron density depends on the Fermi energy: for small fields there is a plateau indicating the presence of the gap, while for higher field this plateau disappears as the gap is closing. Since the fraction of insulating coverage correlates with the magnitude of the resistance, Fig. 10 reproduces the main features of the experimental dependence of the resistance on the gate voltage (Fig. 6), the maximum at the charge neutrality point and the asymmetry. As follows from our calculations, the asymmetry is explained by higher density of states in the valence band compared to the conduction band.

V. DISCUSSION

The influence of magnetic fields on the properties of 2D electrons in HgTe-based quantum wells is a subject of renewed interest since experimental observation of the QSHE state in such systems. We have shown that an in-plane magnetic field B profoundly rebuilds the energy spectrum of 2D electrons in these wells owing to relatively small energy separation of size-quantized subbands. The increase of the field transforms the insulating QSHE state into a gapless metallic state. This theoretical conclusion is supported by experimental data on the disappearance of nonlocal resistance, which takes place around $B = 12$ T in 8-nm-wide wells. The inhomogeneity of the system plays an important role in this phase transition, since it allows formation of the metallic state via percolation at the fields smaller than those predicted theoretically for ideal wells. By considering two plausible mechanisms of disorder, smooth variation of well width and electrostatic potential with reasonable amplitudes, we have calculated the fraction of metallic (p) and insulating ($1 - p$) parts of the sample and found that the percolation threshold, when about half of the 2D plane is in the metallic state ($p \simeq 0.5$), is realized at 10–12 T, in agreement with our experimental data. The dependence of the resistance on the magnetic field and gate voltage qualitatively correlates with the dependence of the insulating fraction on these parameters.

The similarity in behavior of local and nonlocal resistance (Figs. 4 and 5) and persistence of nonlocal resistance up to the field of percolation suggest that the edge state transport remains essential up to the transition to metallic state. Indeed, according to the theory,[14] the in-plane magnetic field does not destroy the edge states. However, the edge states are no longer gapless at any finite B, so that varying the Fermi energy within the bulk gap by the gate one can always reach the situation when the edge state transport is absent. Surprisingly, we do not observe such a behavior in experiment. Another interesting question is how the disorder affects the edge states and their stability. It is generally expected that the physics of topological insulators is unaffected by weak disorder.[1–7] In the presence of in-plane magnetic field, the influence of disorder on the edge state transport should be significant, since we observe a monotonic decrease of nonlocal resistance which becomes stronger as the field approaches the point of phase transition. This behavior could be explained by partial shunting of edge channels by the bulk transport viewed as hopping of electrons between metallic clusters. Indeed, we observe a decrease of both local and nonlocal resistance with temperature (Fig. 5) which can be attributed to increasing probability of such hopping. Another possible mechanism of decrease of nonlocal resistance with increasing B is based purely on the edge state transport properties as described below. The metallic clusters formed at the sample edges can act as additional leads since an electron entering a cluster from the 1D channel is thermalized by dissipation. The presence of additional leads along the path between the voltage probes does not affect the resistance if these leads are assumed to be point-like. However, since the metallic clusters have finite sizes expanding with

increasing B, the effective distance L, which is formed as a sum of all consecutive segments of edge channels connecting the metallic clusters between the voltage probes, decreases. According to Eq. (1), the resistance decreases as well, because at a shorter distance a higher extent of ballisticity is reached.

In conclusion, we have studied the phase transition of a 2D electron system in HgTe quantum wells from the insulating QSHE state to a metallic state which is described as a gapless state according to theory. The transition is caused by application of a magnetic field parallel to the 2D plane. We have emphasized the crucial role of disorder in our samples and discussed the influence of the disorder both on the phase transition and on the edge state transport below the transition field. Whereas our experiments open an interesting possibility for investigating phase transitions in two dimensions, more experimental and theoretical work is required to understand the behavior of 2D electron system in such complex objects as disordered HgTe quantum wells.

ACKNOWLEDGMENTS

Financial support of this work by FAPESP, CNPq (Brazilian agencies), RFBI (N 12-02-00054 and N 13-02-12148-ofi-m), and RAS programs "Fundamental researches in nanostructures and nanomaterials technologies" is acknowledged.

[1] M. Z. Hasan and C. L. Kane, Rev. Mod. Phys. **82**, 3045 (2010); X.-L. Qi and S.-C. Zhang, *ibid.* **83**, 1057 (2011).
[2] X.-L. Qi and S.-C. Zhang, Phys. Today **63**(1), 33 (2010).
[3] J. E. Moore and L. Balents, Phys. Rev. B **75**, 121306 (2007).
[4] J. E. Moore, Nature (London) **464**, 194 (2010).
[5] C. L. Kane and E. J. Mele, Phys. Rev. Lett. **95**, 146802 (2005).
[6] B. A. Bernevig and S. C. Zhang, Phys. Rev. Lett. **96**, 106802 (2006).
[7] B. A. Bernevig, T. L. Hughes, and S. C. Zhang, Science **314**, 1757 (2006).
[8] M. König, S. Wiedmann, C. Brüne, A. Roth, H. Buhmann, L. W. Molenkamp, X.-L. Qi, and S.-C. Zhang, Science **318**, 766 (2007).
[9] A. Roth, C. Brüne, H. Buhmann, L. W. Molenkamp, J. Maciejko, X.-L. Qi, and S.-C. Zhang, Science **325**, 294 (2009).
[10] G. M. Gusev, Z. D. Kvon, O. A. Shegai, N. N. Mikhailov, S. A. Dvoretsky, and J. C. Portal, Phys. Rev. B **84**, 121302(R) (2011).
[11] Z. D. Kvon, E. B. Olshanetsky, D. A. Kozlov, N. N. Mikhailov, and S. A. Dvoretsky, Pis'ma Zh. Eksp. Teor. Fiz. **87**, 588 (2008) [JETP Lett. **87**, 502 (2008)].
[12] Z. D. Kvon, E. B. Olshanetsky, E. G. Novik, D. A. Kozlov, N. N. Mikhailov, I. O. Parm, and S. A. Dvoretsky, Phys. Rev. B **83**, 193304 (2011).
[13] O. E. Raichev, G. M. Gusev, E. B. Olshanetsky, Z. D. Kvon, N. N. Mikhailov, S. A. Dvoretsky, and J. C. Portal, Phys. Rev. B **86**, 155320 (2012).
[14] O. E. Raichev, Phys. Rev. B **85**, 045310 (2012).
[15] S. Das Sarma, S. Adam, E. H. Hwang, and E. Rossi, Rev. Mod. Phys. **83**, 407 (2011).
[16] V. T. Dolgopolov and A. Gold, JETP Lett. **71**, 27 (2000); I. F. Herbut, Phys. Rev. B **63**, 113102 (2001).
[17] S. Das Sarma and E. H. Hwang, Phys. Rev. Lett. **84**, 5596 (2000).
[18] G. Fahsold, A. Priebe, N. Magg, and A. Pucci, Thin Solid Films **428**, 107 (2003).
[19] X. Feng, Y. Deng, and H. W. J. Blöte, Phys. Rev. E **78**, 031136 (2008).